SSRG International Journal of Electronics and Communication Engineering Volume 6 Issue 3, 1-9, March 2019
ISSN: 2348 - 8549 / doi:10.14445/23488549/IJECE-V6I3P101 © 2019 Seventh Sense Research Group®

Improvements in Spectrum Sharing Towards 5G Heterogeneous Networks

Michael Joseph Shundi[*1], Grace Gregory Mihuba[*2], Winnie Griffin Zakayo[*3], Toshtemirov Adkhamjon[*4]

[*1,*2,*4]*Student, School of Information and Communication Engineering, University of Science and Technology Beijing (USTB), Beijing, China.*

[*1]*Instructor, Arusha Technical College, P.O. Box 296, Arusha, Tanzania.*

[*3]*Student, School of Information and Communication Engineering, University of Electronic Science and Technology of China (UESTC), Chengdu, China.*

Abstract

Spectrum frequency is a resource with limited availability, though it is the essential drive to communication systems. The upcoming development of communication networks to upkeep mega-fast broadband services and the underutilization of the licensed spectrum has led to excessive scarcity and henceforth a high demand for the spectrum frequency. This scarcity put importance on the efficient usage of spectrum frequency. However, spectrum sharing between 5G heterogeneous networks is lately being considered to be a resolution to the issue of spectrum frequency scarcity in the future of wireless networks. In this manuscript, we presented the spectrum sharing scenario between collocated overlapped multiple-input multiple-output (MIMO) radar (Overlapped-MIMO radar) and MIMO cellular communication network. We proposed radar antenna arrangement and beam pattern design, which reduces the interference to the MIMO cellular communication network while retaining MIMO radar's performance; specifically, it enhances side-lobe suppression in the beampattern and attains higher signal to noise (SNR) gain. Also, the designed projection sharing algorithm suppresses interference to the MIMO cellular communication network when radar signals are projected onto the communication channel's null space. Simulation results show the MIMO radar's performance when sharing spectrum with the MIMO cellular communication network.

Keywords - *Spectrum frequency, MIMO Cellular Communication networks, Spectrum sharing, Overlapped MIMO Radar. Interference, Radar signal. Null-space projection (NSP), beampattern (s), Overlapped MIMO Radar, Collocated MIMO Radar*

.

I. INTRODUCTION

Spectrum frequency is the most significant resource for wireless communication networks, but its availability is limited[1]. The rapid growth of mobile communication networks to support a wide range of mega-fast broadband services has led to a big capacity demand of the spectrum frequency[2]. The scarcity of spectrum frequency has headed to a new stimulus to search for prominent solutions to make the most efficient use of scarce licensed frequency bands in a shared mode[3]. Spectrum sharing will enhance spectrum utilization efficiency and also save costs to the users of the spectrum[4]. Spectrum sharing between radar and cellular communication networks is an immerging research area aiming to attain more spectrum frequency to meet the high demand for this valuable resource for the upcoming growth of wireless communications networks[1]. It should be noted that existing radar falls between 3 and 100GHz of radio frequency (R.F.) spectrum, which is also the range anticipated by cellular communication networks.

In this paper, the main issues are interference[5] mitigation from the secondary user (SU), which is MIMO cellular communication network to the primary user (PU) (Overlapped MIMO radar and also attaining higher SNR gain[6]. Several ways can be used to achieve spectrum sharing between MIMO radar and MIMO cellular communication network. However, in this paper, we will mostly focus on: proposing antenna arrangement which reduces the interference to the MIMO cellular communication network by enhancing side-lobe suppression in the beampattern and attains higher signal to noise (SNR) gain and also we designed projection sharing algorithm which suppresses interference to the MIMO cellular communication network when radar signals are projected onto null space of the communication channel[7].

The remaining part of this manuscript is structured as follows: Section two (II) presents the sharing scenario between radar and communication network; Section three (III) describes related works previously done by other researchers; Section four (IV) provides the proposed spectrum sharing scenario in details (including proposed antenna arrangement and proposed algorithm); Section five (V) presents simulation results and analysis, and Section six (VI) gives concluding remarks of what has been done in this paper.

II. SHARING SCENARIO BETWEEN RADAR AND CELLULAR COMMUNICATION NETWORK

A. *System Components*

In this section, we are presenting brief descriptions of the sharing system components. The components described here include; radar model, cellular communication model, channel model, and basic assumptions.

a) Radar Model:

We consider a collocated MIMO radar that consisting of M_T transmit and *M.R.* receive antenna elements. The antennas of the collocated MIMO radars are uniform linear array (ULA), and elements are spaced at least a half-wavelength apart (or at the order of half wavelength). Collocated radars are chosen because they provide superior spatial resolution and target parameter identification than widely spaced radar antenna radar[8].

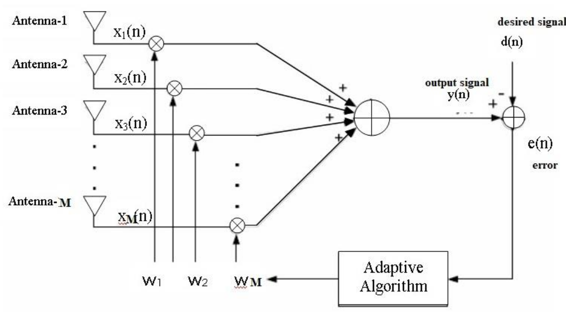

Figure 1: Uniform Linear Array (ULA) diagram [1]

b) MIMO Cellular Communications System Model:

We assume that the communications system is considered a MIMO cellular communication system having N_T transmitted and N_R receive antennas. The communication nodes are considered either base stations (B.S.) or user equipment (U.E.).

c) Channel Model:

The received signal at the receiver terminal of the cellular communications system can be written as

$$y_C(t) = H_I^{N_R \times M_T} X_{Radar}(t) + H^{N_R \times N_T} X_C(t) + n(t) \quad (1)$$

where $X_{Radar}(t)$ is transmitted radar signal, $X_C(t)$ is transmitted cellular communications signal, H_I is $N_R \times M_T$ an interference channel between radar and communications system, H is $N_R \times N_T$ channel between transmitter and receiver of the communications system, $n(t)$ is AWGN.

The interference channel H_I can be denoted as

$$\mathrm{H_I} \triangleq \begin{bmatrix} \mathrm{h_i^{(1,1)}} & \cdots & \mathrm{h_i^{(1,M_T)}} \\ \vdots & \ddots & \vdots \\ \mathrm{h_i^{N_R(,1)}} & \cdots & \mathrm{h_i^{(N_R,M_T)}} \end{bmatrix} (N_R \times M_T) \ \ldots\ldots (2)$$

Where $\mathrm{h_i^{(n,m)}}$ is the coefficient of the channel between m^{th} antenna elements of the MIMO radar to the *n*th antenna element of the MIMO cellular communication networks. The elements of the $\mathrm{H_I}$ are assumed to be independent, identically distributed (i.i.d.), and circularly symmetric complex Gaussian random variables with zero-mean and unit-variance

d) Basic Assumptions

We assumed the radar and cellular communications systems are working in a cooperative R.F. environment, sharing several information while seeking avoidance of interference to each other. In this paper, we investigate a radar-centric design method.

In radar-centric design, we assume that the interference channel state information (CSI) of the communications system is available at the radar terminal. The aim of the radar is then to cultivate its waveform that will mitigate interference to the cellular communications network. A sharing structure is as shown in Figure 1.

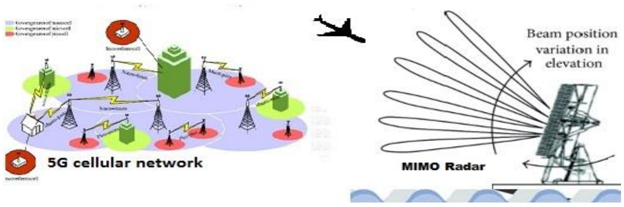

Figure 2: Spectrum sharing scenario between MIMO radar and MIMO cellular communication network.

Further to that, the following assumptions are used all over this paper to make the analysis easy to follow up and instinctive:

=>A point target/source is considered, which is defined for targets/sources having a scatterer with infinitesimal spatial extent.

=> θ and α are deterministic unknown parameters signifying the target's direction of arrival and the complex amplitude of the target, respectively.

=>Path loss α is assumed to be identical for all transmit and receive elements due to the far-field assumption.

=>Angle θ is the azimuth angle of the target.

III. RELATED WORK

The spectrum sharing concept has recently received significant consideration from regulatory bodies and governments worldwide as it seemed to be a promising solution to the great demand for spectrum frequency during the deployment of 5G wireless networks. Observation shows that the traffic increase in cellular wireless communications in recent years, which has been driven by the popularity of a great number of smart devices and Internet-based applications[1], has headed to great capacity demand, which as a result require a solution since the availability of spectrum frequency is limited [9] [10] [11] [12] [13] [14] [15].

For the case of radar sharing spectrum with a cellular communication network, several research has been conducted with several sharing scenarios has been proposed. When radar shares spectrum with a cellular communication network sharing can be achieved by many ways including cooperative sensing approach whereby radar allocated band can be shared with cellular communication system[[16][17]]; a joint communication-radar platform whereby radar can do sensing and only use the unused frequencies; shaping the radar waveforms such that they do not cause interference to the communication system[7].; database aided sensing at the cellular communication network[7], and beamforming approach adjustments can also be deployed at MIMO radar for spectrum sharing[12]. The outcome of mutual interference in the coexistence setup on radar detection and cellular communication system throughput, highlighting some non-trivial interplays and deriving useful design tradeoffs[18]. Some designing of pre-coder of a MIMO-radar spectrally-coexistent with a MIMO cellular system which achieves spectrum-sharing with minimal interference[19]. Weather radar networked system (WRNS) with spectrum sharing among weather radar has been presented. A prototype was also implemented to experiment and explore the feasibility with real weather radar[20]. In [21], a Steepest descent opportunistic MIMO radar was presented in the sight of spectrum sharing. The idea of MIMO radar null space projection (NSP) was first proposed in[7]. The interference of channel null space is computed at the transmitter either by taking advantage of channel reciprocity using its second-order statistics[22] or by blindly approximating the null space, if no cooperation exists between resource sharing nodes [23].

IV. PROPOSED MODEL

A. Spectrum Sharing Between MIMO Radar and MIMO Cellular Communication Network

Taking into consideration the introduction made in section two (II), we now build mathematical bases for collocated MIMO radar, overlapped MIMO radar, performance measures and, Spectrum sharing algorithm.

B. Collocated MIMO Radar:

The considered MIMO radar in this paper is anticipated to be collocated. We define the term ‘collocated’ as a radar system where the transmit and the receive antennas are geographically located closely in space or in the same[24]. The number of antenna elements in the transmits arrays and the receive arrays are M_T and M_R, respectively.

We consider θ *to* be the location parameter of basic target and $\emptyset(t)$ *)* be the waveform emitted from collocated MIMO radar, which can be presented as

$$\emptyset(t) = [\emptyset_1(t)\ \emptyset_2(t)\emptyset_3(t) \ldots \emptyset_{M_T}(t)]^T \quad \ldots\ldots (3)$$

where t is the time dimension of a radar pulse and $(.)^T$ is the transpose of a vector/matrix. The signal $\emptyset_m(t)$, the mth element of the vector $\emptyset(t)$, is the waveform emitted by the mth transmit antenna of the MIMO radar.

In this scenario, signals transmitted by each antenna element are considered to be orthogonal to each other. Therefore, satisfying the orthogonality principle, this deduces;

$$R_x = \int_{T_0} \emptyset(t)\emptyset^H(t)dt = I_{M_T} \quad \ldots\ldots(4)$$

Where T_0 stands for the radar pulse width, $(.)^H$ denotes the Hermitian transpose, and I_{M_T} is the $M_T \times M_T$ identity matrix.

However, at the transmitter, the waveform is steered toward the direction of a particular target during transmission. Assuming the target direction to be θ and $M_T \times 1$, and transmit steering vector $a(\theta)$, then for a uniform linear array (ULA), the transmit steering vector $a(\theta)$ can be presented as

$$a(\theta) = [a_1(\theta)a_2(\theta)a_3(\theta) \ldots a_{M_T}(\theta)]^T \quad \ldots\ldots(5)$$
$$= [1 e^{-j2\pi d_T sin\theta} \ldots e^{-j2\pi d_T (M_T-1) sin\theta}]^T$$

Where the first element of the vector $a(\theta)$ is considered as the reference element, which is set as $a_1(\theta) = 1$, the mth element is set as $a_m(\theta) = e^{-j2\pi d_T (M_T-1) sin\theta}$, and the inter-element space for the array is denoted as d_T (in terms of wavelength). Therefore, the initial waveform is multiplied with the steering vector, and the final output of the radar transmitter can be stated in compacted vector form as

$$X_{Radar} = a(\theta) \odot \emptyset(\mathrm{t}) \quad \ldots\ldots (6)$$
$$= [a_1(\theta)\emptyset_1(t)\ \ a_2(\theta)\emptyset_2(t)\ \ a_3(\theta)\emptyset_3(t) \ldots a_{M_T}(\theta)\emptyset_{M_T}(t)]$$
$$= [x_1(t)\ \ x_2(t)\ \ x_3(t) \ldots x_{M_T}(t)]$$

Where $\odot$ denotes the element-wise product. The snapshot vector of size $M_R \times 1$ received by the collocated MIMO radar receive antenna array can be presented as;

$$y_{Radar}(t) = y_s(t) + y_i(t) + n(t) \quad \ldots\ldots (7)$$

Where $y_s(t)$ is the signal from the target/source, $y_i(t)$ is the jamming/interference signal, and $\boldsymbol{n}(t)$ is the AWGN. If a single point target/source is assumed, then the received signal at the radar converts to

$$y_s(t) = \beta_s\big(a^T(\theta_s)\emptyset(t)\big)\mathbf{b}(\theta_s) \quad \ldots\ldots (8)$$

where θ_s is the direction of the target/source, β_s is the complex-valued reflection coefficient of the focal point θ_s , and $\mathbf{b}(\theta)$ is the receive steering vector of size $M_R \times 1$ for the direction θ, which can be presented as

$b(\theta) = [b_1(\theta) b_2(\theta) b_3(\theta) \dots b_{M_R}(\theta)]^T$ ……..(9)
$= [1 e^{-j2\pi d_T sin\theta} \dots . e^{-j2\pi d_T (M_R - 1) sin\theta}]^T$

The signal returned from the *m*th transmitted waveform can be recovered by implementing a matched-filter at the receiver of the radar. The matched-filter would contain each of the waveforms $\{\emptyset_m(t)\}_{m=1}^{M_T}$ and will be matched with the received signal as following

$\boldsymbol{y_m}(t) = \int_{T_0} \boldsymbol{y_{Radar}}(t) \emptyset_m^*(t) dt \quad m = 1, \dots . . M_T$ … ……(10)

Normally, MIMO radar does have more degrees of freedom by the rise of the virtual array. Taking into account that the transmitting signals from the single transmitter of the radar are different. Therefore, the echo signals can be re-assigned to the source. As a result, gives an enlarged virtual receive aperture. Then, the size of the virtual data vector will be $M_T M_R \times 1$, and it can be presented as

$y_v = [y_1^T \; y_2^T \; y_3^T \dots . y_{M_T}^T]^T$ …………….(11)
$= \beta_s a(\theta_s) \otimes b(\theta_s) + y_{i+n}$

Where $\otimes$ denotes the Kronker product operator and y_{i+n} denotes the combined component of interference and noise. Therefore, the target/source signal component can be presented as

$y_s = \beta_s V(\theta_s)$ ………(12)

where $V = a(\theta_s) \otimes b(\theta_s)$ is the virtual steering vector of size $M_T M_R \times 1$, which is associated with a virtual array of $M_T M_R$ elements.

For ULA, the $(m_t M_R + m_r)th$ entry of the virtual array steering vector $V(\theta)$ is given by
$V_{[m_t M_R + m_r]}(\theta) = e^{-j2\pi(m_t d_T sin\theta + m_r d_R sin\theta)}$ …. (13)

Where $m_t = 0 \dots, M_T - 1$, and $m_r = 0 \dots, M_R - 1$. For $d_T = M_R d_R$, the virtual array steering vector simplified to [10]
$V_{[\varsigma]}(\theta) = e^{-j2\pi\varsigma d_R sin\theta}$ …………..(14)

where $\varsigma = m_t M_R + m_r = 0,1, \dots M_T M_R - 1$ which infers that an $M_T M_R$ effective aperture array can be achieved by employing $M_T + M_R$ antennas [5]. Here, the resulting virtual array is a ULA of M_T M_R elements spaced and d_R wavelength apart. For collocated MIMO radar, aperture size increases due to virtual array, which is resulted from the use of orthogonal signals in the antenna elements. This size extension is referred to as *waveform diversity*.

C. Overlapped-MIMO Radar

In this scenario, the antenna elements of the array are partitioned into multiple overlapped sub-arrays. One important advantage is that this formulation allows to beamform in both transmit and receive arrays. Conceptually, we partition the transmit arrays into K sub-arrays where $1 \le K \le M_T$ which are permitted to overlap [25]. The Overlapped-MIMO radar formulation is shown in Figure 2.

The complex envelope of the signals at the output of the *k*th subarray can be presented as

$S_k(t) = \sqrt{\frac{M_T}{K}} \emptyset_k(t) \widetilde{\omega}_k \quad k = 1, \dots . , K$ ……………… …(15)

where $\widetilde{\omega}_k$ is a $M_T \times 1$ unit-norm complex vector with M_k beamforming weights matching to the active antenna elements in *k*th sub-array and $M_T - M_k$ zero weights corresponding to the inactive antennas.

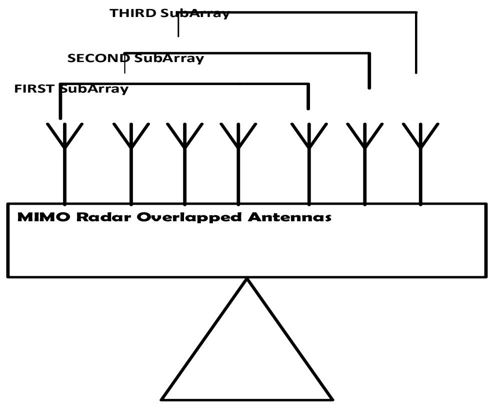

Figure 3: Overlapped MIMO Radar Antenna formulation

As a transmitted signal, the frequency spaced signals can be adopted [26], which is orthogonal if the frequency increment $\Delta f = f_{k+1} - f_k$ between the waveform $\emptyset_k + 1$ to $\emptyset_k$ satisfies $\Delta f \gg 1/T_0$. The orthogonal waveform $\emptyset(t)\;_k$ can be modeled as
$\emptyset_k(t) = Q(t) e^{j2\pi k(\Delta f)t}$ ………… (16)
where *Q(t)* is the pulse shape of duration *T*0, where $0 < t < T_0$, and *k=1,…K* [26].
The energy of $S_k(t)$ within one radar pulse can be written as
$E_k = \int_{T_0} S_k^H(t) S_k(t) dt = \frac{M_T}{K}$ ……. (17)
Which deduces that the total transmitted power is equal to M_T . The reflected signal from the target/source at the direction θ in the far-field can be expressed as

$r(t,\theta) \triangleq \sqrt{\frac{M_T}{K}} \beta(\theta) \sum_{k=1}^{K} \widetilde{\omega}_k^H \tilde{a}_k(\theta) \emptyset_k(t)$ …… (18)

$= \sqrt{\frac{M_T}{K}} \beta(\theta) \sum_{k=1}^{K} \omega_k^H a_k(\theta) e^{-j\tau_k(\theta)} \emptyset_k(t)$

Where $\beta(\theta)$ is the reflection coefficient, ***w****k*, and $a_k(\theta)$ are the $M_k \times 1$ beamforming vectors and steering vector, respectively. The $\tilde{a}_k$ is a $M_T \times 1$ vector with M_k steering vector matching to the active antenna elements in *k*th subarray and $M_T - M_k$ zero corresponding to the inactive antennas. As a result, $T_k(\theta)$ is the time of propagation required for the wave to travel from the first element to the next element.
The Equation (18) can be rewritten as

$$r(t,\theta) \triangleq \sqrt{\frac{M_T}{K}}\beta(\theta)(c(\theta)\odot d(\theta))^T \emptyset_K(t) \;\ldots\ldots\; (19)$$

where the waveform vector is
$\emptyset_K(t) \triangleq [\emptyset_1(t), \ldots \emptyset_K(t)]$,
With dimension $K \times 1$, the transmit coherent processing vector is $c(\theta) \triangleq [w_1^H a_1(\theta), \ldots w_K^H a_K(\theta)]$ with dimension $K \times 1$, and the waveform diversity vector is $d(\theta) \triangleq [e^{-jT_1(\theta)}, \ldots e^{-jT_K(\theta)}]$ with dimension $K \times 1$. The received complex vector of the array observation can be presented as

$$y_{Radar}(t) = r(t,\theta_s)b(\theta_s) + \sum_i^D r(t,\theta_i)b(\theta_i) + n(t), \;\ldots\ldots (20)$$

Where D is the number of interfering signals (or scatterers), $\mathbf{b}(\theta)$ is the receive steering vector of size $M_R \times 1$ associated with direction θ, and $\boldsymbol{n}(t)$ is AWGN. Following Equation (10) and (11), by match-filtering $\boldsymbol{y_{Radar}(t)}$ to each of the waveforms, $\{\emptyset_k\}_{k=1}^K$ we can obtain $KM_R \times 1$ virtual data vectors as

$$y_v = [y_{Radar}^T, 1^{(t)} \ldots y_{Radar}^T, K^{(t)}]^T \;\ldots\ldots (21)$$
$$= \sqrt{\frac{M_T}{K}}\beta_s \boldsymbol{u}(\theta_s) + \sum_i^D \sqrt{\frac{M_T}{K}}\beta_i \boldsymbol{u}(\theta_i) + \boldsymbol{n},$$

Where $\mathbf{u}(\theta) \triangleq [(\mathbf{c}(\theta)\odot \mathbf{d}(\theta)) \otimes \mathbf{b}(\theta)]$ is the $KM_R \times 1$ virtual steering vector, $\beta_s = \beta(\theta_s)$ and $\beta_i = \beta(\theta_i)$ are the reflection coefficients of the target/source and interference, respectively. This overlapped sub-array formulation collapses to a phased array when $K = 1$ is chosen. In this scenario, only one waveform is emitted. This leads to lower angular resolution but higher coherent processing gain, like phased-array radar. Likewise, when $K = M_T$ is chosen, the formulation becomes a conventional MIMO without array partition. This totally reduces coherent processing gain but results from higher angular resolution.

D. *Performance Measures for Overlapped-MIMO Radar*

In this part, performance measures of the proposed null space projected Overlapped-MIMO radar waveform. We evaluate the performance of the proposed architecture based on beampattern and SNR gain computation. Starting with computing the corresponding beamformer weight vector. In the case of non-adaptive beamforming, the analogous beamformer weight vectors are given for the *k*th transmitting subarray as

$$w_k = \frac{a_k(\theta_s)}{\|a_k(\theta_s)\|} = \frac{a_k(\theta_s)}{\sqrt{M_T-K+1}} \;\ldots\ldots\ldots (22)$$

where $k = 1, 2, \cdot\ \cdot\ \cdot, K$. The beamforming weight vector of size $K.N. \times 1$ for the receiving subarrays can be written as

$$w_d \triangleq u(\theta_s) = [c(\theta_s)\odot d(\theta_s)] \otimes b(\theta_s) \;\ldots\ldots (23)$$

a) Beampattern Improvement

Let $G(\theta)$ be the normalized overall beam pattern for Overlapped-MIMO

$$G(\theta) = \frac{|w_d^H u(\theta)|^2}{|w_d^H u(\theta_s)|^2} = \frac{|u^H(\theta_s)u(\theta)|^2}{\|u(\theta_s)\|^4} \;\ldots\ldots\ldots (24)$$

For the distinctive case of a ULA, we have $a_1^H(\theta)a_1(\theta_s) = \cdots = a_K^H(\theta)a_K(\theta_s)$ Utilizing Equation (24), the beam pattern of the Overlapped-MIMO radar for a ULA with overlapped partitioning of K transmit subarrays can be expressed as;

$$G_0(\theta) = \frac{|a_K^H(\theta_s)a_K(\theta)[(d(\theta_s)\otimes b(\theta_s))^H(d(\theta)\otimes b(\theta)]|^2}{\|a_K^H(\theta_s)\|^4 \|d(\theta_s)\otimes b(\theta_s)\|^4} \;\ldots\ldots (25)$$

As we know that $\|a_K(\theta_s)\|^2 = M_T - K + 1$ $\|d(\theta_s)\|^2 = K$ and $\|b(\theta_s)\|^2 = M_R$, the overall beam pattern can be expressed as

$$G_0(\theta) = \frac{|a_K^H(\theta_s)a_K(\theta)|^2}{(M_T-K+1)^2}\cdot\frac{|d^H(\theta_s)d(\theta)|^2}{K^2}\cdot\frac{|b^H(\theta_s)b(\theta)|^2}{M_R^2}, \ldots\ldots (26)$$
$$T_0(\theta)\cdot D_0(\theta)\cdot R(\theta)$$

Where the waveform diversity beam pattern is $D_0(\theta) \triangleq \frac{|d^H(\theta_s)d(\theta)|^2}{K^2}$, the transmit beam pattern is $T_0(\theta) \triangleq \frac{|a_K^H(\theta_s)a_K(\theta)|^2}{(M_T-K+1)^2}$, and the receive beam pattern is $R(\theta) \triangleq \frac{|b^H(\theta_s)b(\theta)|^2}{M_R^2}$. So, we can see that the overall beam pattern of the Overlapped-MIMO radar can be expressed in terms of three separate and independent beampattern:-

For MIMO radar, the subarray number is $K = M_T$ and the transmitter beampattern $T_M(\theta) = 1$. Hence, the overall beam pattern for MIMO radar can be expressed as

$$G_{MIMO}(\theta) = D_M(\theta)\cdot R(\theta) \;\ldots\ldots (27)$$

where the waveform diversity beampattern is $D_M(\theta) = \frac{|a^H(\theta_s)a(\theta)|^2}{M_T^2}$. Taking into account that the overall beam pattern of the MIMO radar has only the waveform diversity and receive beam pattern.

For phased-array radar, the subarray number is $K = 1$ and the waveform diversity beampattern $D_P(\theta) = 1$; therefore, the overall beam pattern for phased-array radar can be expressed as

$$G_{PH}(\theta) = T_P(\theta).R(\theta) \;\ldots\ldots (28)$$

where the transmit beampattern is $T_P(\theta) = \frac{|a^H(\theta_s)a(\theta)|^2}{M_T^2}$. Taking into account that the overall beam pattern of the phased-array radar has only transmit and receive beam pattern.

b) SNR Gain Improvement

According to [5], the output SNR of the Overlapped-MIMO radar with non-adaptive transmit/receive beamforming can be expressed as

$$SNR_{OMIMO} = M_R M_T (M_T - K + 1)\frac{\sigma_s^2}{\sigma_n^2} \;\ldots\ldots(29)$$

where σ_s^2 is the variance of the target/source reflection coefficient, thus $\sigma_s^2 = E\{|\ \beta\ |^2\}$, and σ_n^2 is the noise variance.

For MIMO radar, the output SNR can be found by substituting $K = M.T.$ at Equation (29)

$$SNR_{MIMO} = M_R M_T \frac{\sigma_s^2}{\sigma_n^2} \ \ldots.. (30)$$

For phased-array radar, the output SNR can be found by substituting $K = 1$ at Equation (29)

$$SNR_{PH} = M_R M_T^2 \frac{\sigma_s^2}{\sigma_n^2} = M_T \cdot SNR_{MIMO} \ \ldots... (31)$$

Finally, from Equation (29) – (31), we can express the output SNR of Overlapped-MIMO radar as

$$SNR_{OMIMO} = \eta \cdot SNR_{PH} = \eta \cdot M_T \cdot SNR_{MIMO} \quad \ldots. (32)$$

where $\frac{1}{M_T} \leq \eta \triangleq \frac{M_T - K+1}{M_T} \leq 1$ is the ratio between the overlapped-MIMO radar SNR gain and that of the phased-array radar.

We can observe that the SNR gain of the MIMO radar is equal to $M_R M_T$ and the SNR gain of the phased-array radar is equal to $M_R M_T^2$, and the SNR gain of the Overlapped- MIMO radar is equal to $M_R M_T (M_T K + 1)$. The SNR gain of the phased-array radar is $\square_T$ times greater than that of the MIMO radar. The SNR gain of the Overlapped- MIMO radar is $(M_T K + 1)$ times greater than that of the MIMO radar and $\frac{(M_T K+1)}{M_T}$ times greater than that of the phased-array radar. Hence, we can see an overall SNR gain improvement for the Overlapped-MIMO architecture.

E. Optimum Subarray Size for Overlapped-MIMO Radar

For the sake of maximizing the impact of the overlapping subarray architecture presented, we have to choose a value for the number of subarrays K that maximizes the virtual array size M_ϵ. Hence,

$$K = \arg\max_K (M_\epsilon) \ \ldots.. (33)$$

Where $M_\epsilon = (M_T - K + 1)K$.

The number of subarrays K in the overlapped array can be optimized by

$$\frac{\partial}{\partial K}(M_\epsilon) = 0 \ldots... (34)$$

$$\frac{\partial}{\partial K}\big((M_T - K + 1)K\big) = 0$$

$$M_T - 2K + 1 = 0$$

$$K = \left\lfloor \frac{M_T+1}{2} \right\rfloor$$

Where $\lfloor\cdot\rfloor$ stands for the floor operation as K should be an integer. Take into account that the radar has the most important impact when the number of virtual arrays $M_\epsilon$on the transmitter side is maximized (see Equation (34)).

F. Algorithm for Radar-Centric Spectrum Sharing

In this part, we present the projection algorithm, which projects the Overlapped-MIMO radar signal onto the null space of the communication interference channel via the null space projection (NSP) technique proposed in [1]. We start with a basic explanation of the spectrum sharing algorithm and move on to present the numerical details of the projection matrix.

a) Null Space Projection (NSP):

In this part, we present the null-space projection (NSP) algorithm, which projects the radar signal onto the null space of the interference channel **H.I.**. The NSP algorithm requires the radar to have the interference channel's CSI available in advance, which can be found in a number of ways and transported to the radar via mutual cooperation between the radar and the cellular communication network[1].

This is how the projection algorithm works. First, the radar receives **H.I.**, which is the CSI between radar and communication node's interference channel. It then computes the number of null spaces available to project the radar signal by performing singular value decomposition (SVD) on **H.I.**. The dimension of the null space is$M_T - N_R$. It then computes the projection channel matrix **P** and constructs a new radar waveform$\widehat{\mathbf{X}}_{\mathbf{Radar}}$. If $\mathbf{H_I}$ is the channel matrix and **P** is the projection matrix onto the null space of **H.I.**, then the overlapped-MIMO radar waveform projected onto the null space of **H.I.** to avoid interference from the radar can be written as

$$\widehat{\mathbf{X}}_{\mathbf{Radar}} = \mathbf{P}_{\mathbf{X}_{\mathbf{Radar}}}(\mathrm{t}) \ \ldots.. (35)$$

Take into account that the spectrum sharing algorithm via null space projection (NSP) described above is shown in Algorithm 1.

b) Projection Matrix:

In this part, we present the creation of the projection matrix **P** and analyze the properties of this projection matrix. Let $\mathbf{H_I}$ be the interference channel between the radar and cellular communications node. We consider that, $\mathbf{H_I} \in \mathbf{F}^{\mathbf{N_R} \times \mathbf{M_T}}$ for $\mathbf{F} = \mathbb{R}$ or $\mathbf{F} = \mathbb{C}$. We need a projection matrix $\mathbf{P} \in \mathbf{F}^{\mathbf{M_T} \times \mathbf{M_T}}$ of a maximum rank such that it satisfies fowling properties:

$$\mathbf{H_I P = 0}$$

$$\boldsymbol{P^2 = P}$$

Algorithm 1 Spectrum Sharing Algorithm via Null Space Projection (NSP)

loop

Get CSI of **H.I.** through feedback from 'Communications Node'..

Send $\mathbf{H_I}$ to inner loop (i.e., NSP Algorithm) for projection matrix **P** formation.

if H.I. received from the outer loop, **then**

Perform SVD on **H.I.** **(i.e.** $H_I = U\Sigma V^H$)

Construct $\tilde{\Sigma} = diag(\widetilde{\sigma_1}, \widetilde{\sigma_2}, \ldots, \widetilde{\sigma_k})$

Construct$\tilde{\Sigma}' = \tilde{\sigma}_1', \tilde{\sigma}_2' \ldots.., \tilde{\sigma}_{\mathbf{M_T}}')$

Setup projection matrix $P = V\tilde{\Sigma}' V^H$

Send **P** to the outer loop.

end if
Receive the projection matrix **P** from the inner loop.
Perform null space projection, i.e.,
$\widehat{\mathbf{X}}_{\mathbf{Radar}}(t) = \mathbf{P}_{\mathbf{X}_{\mathbf{Radar}}}(\mathrm{t})$
end loop

The projection matrix **P**, which satisfies the above properties and projects onto the null space of interference channel **H.I.**, can be found by taking the SVD of **H.I**. The SVD of **H.I.** is

$H_I = U\Sigma V^H$ .....(36)
where **U** and **V** are unitary or orthogonal, depending on **F**, of order $\mathbf{N_R}$ and $\mathbf{M_T}$, respectively, and $\Sigma \in \mathbb{R}^{\mathbf{N_R}\times\mathbf{M_T}}$ is and $\mathbf{N_R} \times \mathbf{M_T}$ rectangular diagonal matrix with non-negative real numbers on the diagonal. Let us define

$\tilde{\Sigma} = diag(\tilde{\sigma_1}, \tilde{\sigma_2}, \ldots, \tilde{\sigma_k})$ ..... (37)
Where $k = \min(N_R, M_T)$ and $\tilde{\sigma_1} \geq \tilde{\sigma_2} \geq \cdots \geq \tilde{\sigma_p} \geq \widetilde{\sigma_{p+1}} = \widetilde{\sigma_{p+2}} = \cdots = \tilde{\sigma_k} = 0$
are the singular values of **H.I**. Let us define

$\tilde{\Sigma}' = \tilde{\sigma}_1', \tilde{\sigma}_2' \ldots, \tilde{\sigma}_{\mathbf{M_T}}')$ ..... (38)
Where $\tilde{\Sigma}' \in \mathbb{R}^{\mathbf{M_T}\times\mathbf{M_T}}$ and
$\tilde{\sigma}_i' = \begin{cases} 0, if\ i \leq p, \\ 1, if\ i > p. \end{cases}$
Note that, $\tilde{\Sigma}\tilde{\Sigma}' = 0$ and $(\tilde{\Sigma}')^2 = \tilde{\Sigma}'$. Now, one can define the projection matrix
$P = V\tilde{\Sigma}'V^H$ ...... (39)
We can prove that this matrix **P** is a valid projection matrix by computing the properties mentioned above. The details of these proofs are given below.

Property 4.1 $\mathbf{P} \in \mathbb{R}^{\mathbf{N_R}\times\mathbf{M_T}}$ *is an orthogonal projection matrix onto the null space of* $\boldsymbol{H_I} \in \mathbb{R}^{\mathbf{N_R}\times\mathbf{M_T}}$, *if and only if* $H_I P = H_I P^H = 0$.

Proof Since $P = P^H$ (see property 2), it can be written
$H_I P = H_I P^H = U\tilde{\Sigma}V^H \times V\tilde{\Sigma}'V^H = 0$ ..... (40)
The result mentioned above follows from the fact that $\tilde{\Sigma}\tilde{\Sigma}' = 0$ by construction.

Property 4.2 $\mathbf{P} \in \mathbb{R}^{\mathbf{N_R}\times\mathbf{M_T}}$ *is a projection matrix, if and only if* $P = P^H = P^2$.
Proof At first, let us prove the 'only if' part, where we will have to prove $P = P^H$. By taking the Hermitian of Equation (39), we will get
$P^H = (V\tilde{\Sigma}'V^H)^H = P$ ...... (41)
Then, by squaring the Equation (39), we will get
$P^2 = V\tilde{\Sigma}V^H \times V\tilde{\Sigma}V^H = P$ ..... (42)
where Equation (42) follows from $V^H V = I$ (both of them are orthonormal matrices) and $(\tilde{\Sigma}')^2 = \tilde{\Sigma}'$ (by construction). If we follow Equations (41) and (42), we will find that $P = P^H = P^2$

Next, we will show that **P** is a projector matrix by proving that if **V** ∈range (**P**), then **Pv=v**, i.e., for some **w**, **v=Pw**, then
$Pv = P(Pw) = P^2 w - Pw = v$ .... (43)
On top of that, $Pv - v \in null(P)$, i.e.,
$P(Pv - v) = P^2 v - Pv = Pv - Pv = 0$ .....(44)
This concludes the proof.

F. *Limiting Factors and Assumptions of NSP*

We consider two (2) spectrum sharing scenarios depending upon the number of antenna elements in the radar and cellular communications system. The main assumption of NSP algorithm execution is 'cooperation'. There has to be a certain kind of cooperation between the radar and the communication node to project radar signal onto the null space efficiently. They have to be exchanging the CSI of the inference channel through feedback/feedforward or any other kind of mechanism. It will work only when the channel is fixed or quasi-static, meaning the CSI will not be altered before the projection occurs. Ways to exchange CSI between radar and communications system is presented in [1].

Take into account that we run into two possible cases: (1) the number of antenna elements in radar transmit array is less than equal to that of the communications system, $\mathbf{M_T} \leq \mathbf{N_R}$ and (2) the number of antenna elements in the radar transmit array is greater than that of the communications system, $\mathbf{M_T} > \mathbf{N_R}$ For the first case where we have $\mathbf{M_T} \leq \mathbf{N_R}$, we cannot use the NSP technique. However, a possible way out to this problem is using Overlapped-MIMO as it increases the effective number of transmit arrays, thus making NSP possible. In this case, the effective transmit array aperture M_ϵ is equal to $(M_T - K + 1)K$, which is greater than $\mathbf{N_R}$. Note that M_ϵ is fundamentally the number of the virtual arrays in the transmitter of the radar. Therefore, the Overlapped-MIMO radar fallouts in a total virtual array of size$((M_T - K + 1)K)M_R$. Also, if $\mathbf{M_T} > \mathbf{N_R}$, then we will have enough degrees of freedom (DoF) to make NSP possible for $\mathbf{M_T} - \mathbf{N_R}$ dimensions. Conversely, even in this case, the performance can be increased using Overlapped-MIMO since it rises the effective number of transmit arrays.

V. RESULTS AND ANALYSIS

In this part, we present we simulation performance of an Overlapped-MIMO radar.

Assumptions:
=>ULA with $M_T = 20$ antenna elements at the transmitter and also $M_R = 20$ antennas at the receiver.
=>In both scenarios, the space between elements is $d_T = 0.5$ (=half wavelength).
=>The signal passes through a Rayleigh distributed channel and is subject to AWGN.
=>Each antenna element is omnidirectional.
=>The target of interest is at $\theta_s = 15^0$ and;

=> To simplify, we ignored the presence of any interfering signals in here. Moreover, output SNRs are computed using 10,000 independent simulations.

Figure 4 reveals the overall beam pattern for four different MIMO radar constructions: (1) Overlapped-MIMO radar with $K = 1$ (single subarray or phased-array), (2) Overlapped-MIMO radar with K = 5, (3) Overlapped-MIMO radar with K = 10, and (4) MIMO radar with K = 20 (MIMO). Here the Overlapped-MIMO radars have two different orientations of 5 and 10 overlapped subarrays, and each subarray has 11 and 16 antenna elements, respectively. We can observe that the Overlapped- MIMO with K = 1 (phased-array) and MIMO radars have precisely the same overall transmit/receive beampatterns. However, the Overlapped-MIMO radar (for K =5 and K = 10) has significantly enhanced side-lobe suppression equated to the beampattern
of the MIMO and the phased-array radar.

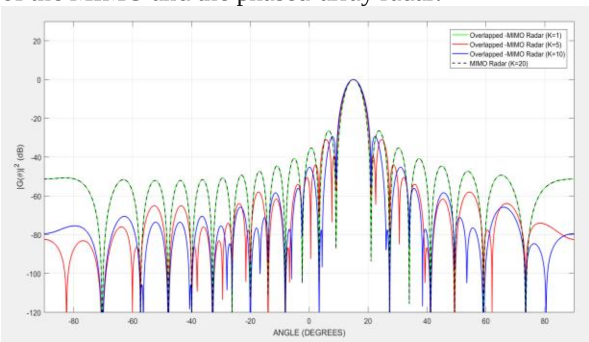

Figure 4: General beampattern using conventional transmit-receive beamformer where the total number of elements is M_T = 20, the number of overlapped sub-arrays is K = 5 and K = 10, respectively; the number of elements in each sub-array is $(M_T - K + 1) = 16$ and $(M_T - K + 1) = 11$, respectively, and $d_T = 0.5$ wavelength

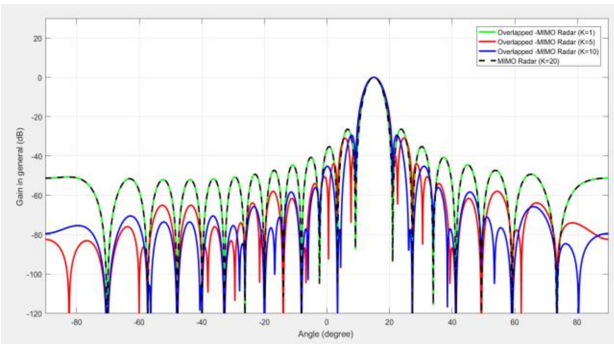

Figure 5: General beampattern using conventional transmit-receive beamformer and NSP where the total number of elements is M_T = 20, the number of overlapped sub-arrays is K = 5 and K = 10, respectively; the number of elements in each sub-array is $(M_T - K + 1) = 16$ and $(M_T - K + 1) = 11$, respectively, and $d_T = 0.5$ wavelength

Figure 5 reveals the general beampattern for same radar formulations with NSP algorithm: (1) Overlapped-MIMO radar with K = 1 plus NSP (single subarray or phased-array), (2) Overlapped-MIMO radar with K = 5 plus NSP, (3) Overlapped-MIMO radar with K = 10 plus NSP, and (4) MIMO radar with K = 20 plus NSP (MIMO). We perceive that the projection algorithm has reduced side-lobe mitigation as expected. Note that it is still providing encouraging suppression in comparison to pure MIMO radar. However, the primary benefits are at the cellular communications side since this NSP algorithm minimizes interference from the radar to the communications system and thus, enables the two to coexist.

The last experiment considers the number of sub-arrays, K, in the transmitter of the Overlapped-MIMO radar that enlarges the benefit for the radar in terms of side-lobe elimination. Take into account that the radar has the most important effect when the number of virtual arrays M_ϵ on the transmitter side is reduced (Equation (34)).

Figure 5 shows the impact of varying the number of sub-arrays K from 1 to M_T on M_ϵ. For $M_T = 20$, K = 11, or K = 12 results in the highest effect. This information aids in determining the structure of overlapping sub-arrays. The plot of K for $M_T = 10$ and $M_T = 15$ is presented in the same figure to provide a comparative view. This graph aids in picking a value for K (the number of sub-arrays in the Overlapped-MIMO structure) that increases the virtual antenna array size, thus enhancing the amount of side-lobe suppression in radar beam pattern while retaining the dimension needed for NSP.

VI. CONCLUSION

Spectrum sharing in heterogeneous networks is much expected to be the answer to the problem of scarcity of spectrum frequency resources. This scarcity of spectrum frequency is basically due to bandwidth demand for future wireless communication (5G) and the underutilization of the licensed spectrum frequency, which is currently in use. The sharing of the spectrum not only will enhance the use of the licensed spectrum frequency but also will save cost(s) to the users of the spectrum and increase the capacity of the communication networks. However, the spectrum sharing between radar and communication networks is now getting a high consideration as one of the areas for spectrum sharing in 5G wireless communication networks. In this manuscript, we showed the spectrum sharing scenario between collocated overlapped multiple-input multiple-output (MIMO) radar (Overlapped-MIMO radar) and MIMO cellular communication network. We proposed radar antenna arrangement and beampattern design, which reduced the interference to the MIMO cellular communication network while retaining the performance of MIMO radar; specifically, it enhanced side-lobe suppression in the beampattern and attained higher signal to noise (SNR) gain. Also, the designed projection sharing algorithm suppressed interference to the MIMO cellular communication network when radar signals are projected onto the null space of the communication channel. Simulation results showed the analysis of the MIMO radar the performance when sharing spectrum with MIMO cellular communication network.

Funding: This study was funded by the "Beijing Institute of Technology Research Fund Program for Young Scholars."

REFERENCES

[1] M. J. Shundi, I. Iddi, G. Gregory, and M. Toshtemirov, "ENHANCING THE EFFICIENCY OF LICENCED SPECTRUM SHARING IN 5G HETEROGENEOUS NETWORKS," Int. Res. J. Eng. Technol., vol. 06, no. 03, pp. 1106–1119, 2019.

[2] M. J. Shundi and E. T. A. Mwangela, "A Review on Coordination Techniques for Licensed Spectrum Sharing in 5G Networks," J. Netw. Commun. Emerg. Technol., vol. 8, no. 9, pp. 16–25, 2018.

[3] B. Zhong, Z. Zhang, and S. Member, "Secure Full-Duplex Two-Way Relaying Networks With Optimal Relay Selection," vol. 21, no. 5, pp. 1123–1126, 2017.

[4] C. Yang, J. Li, M. Guizani, A. Anpalagan, and M. Elkashlan, "Advanced spectrum sharing in 5G cognitive heterogeneous networks," IEEE Wirel. Commun., vol. 23, no. 2, pp. 94–101, 2016.

[5] M. J. Shundi and G. G. Mihuba, "Improved Diagonal Loading for Robust Adaptive Beamforming Based On LS-CMA," Int. J. Emerg. Technol. Eng. Res., vol. 6, no. 8, pp. 19–29, 2018.

[6] A. Khawar, A. Abdel-hadi, T. C. Clancy, and R. Mcgwier, "Beampattern Analysis for MIMO Radar and Telecommunication System Coexistence," no. 1, pp. 534–539, 2014.

[7] S. Sodagari, A. Khawar, T. C. Clancy, and R. McGwier, "A projection based approach for radar and telecommunication systems coexistence," GLOBECOM - IEEE Glob. Telecommun. Conf., pp. 5010–5014, 2012.

[8] J. Li and P. Stoica, "MIMO Radar with Colocated Antennas," IEEE Signal Process. Mag., vol. 24, no. 5, pp. 106–114, 2007.

[9] S. S. Bhat, R. M. Narayanan, and M. Rangaswamy, "Bandwidth sharing and scheduling for multimodal radar with communications and tracking," Proc. IEEE Sens. Array Multichannel Signal Process. Work., pp. 233–236, 2012.

[10] I. Repository, "Network visualization : a review," vol. 2, no. 6, pp. 856–868, 2007.

[11] Z. Geng, H. Deng, and B. Himed, "Adaptive radar beamforming for interference mitigation in radar-wireless spectrum sharing," IEEE Signal Process. Lett., vol. 22, no. 4, pp. 484–488, 2015.

[12] H. Deng and B. Himed, "Interference mitigation processing for spectrum-sharing between radar and wireless communications systems," IEEE Trans. Aerosp. Electron. Syst., vol. 49, no. 3, pp. 1911–1919, 2013.

[13] B. M. J. Marcus and D. Sc, "New Approaches to Private Sector Sharing of Federal Government Spectrum," no. June, 2009.

[14] M. Rihan and L. Huang, "Optimum Co-Design of Spectrum Sharing between MIMO Radar and MIMO Communication Systems: An Interference Alignment Approach," IEEE Trans. Veh. Technol., vol. 67, no. 12, pp. 11667–11680, 2018.

[15] M. P. Fitz, T. R. Halford, I. Hossain, and S. W. Enserink, "Towards simultaneous radar and spectral sensing," 2014 IEEE Int. Symp. Dyn. Spectr. Access Networks, DYSPAN 2014, pp. 15–19, 2014.

[16] C. Sturm and W. Wiesbeck, "Waveform design and signal processing aspects for fusion of wireless communications and radar sensing," Proc. IEEE, vol. 99, no. 7, pp. 1236–1259, 2011.

[17] F. Paisana, J. P. Miranda, N. Marchetti, and L. A. Dasilva, "Database-aided sensing for radar bands," 2014 IEEE Int. Symp. Dyn. Spectr. Access Networks, DYSPAN 2014, pp. 1–6, 2014.

[18] R. Saruthirathanaworakun, J. M. Peha, and L. M. Correia, "Performance of data services in cellular networks sharing spectrum with a single rotating radar," 2012 IEEE Int. Symp. a World Wireless, Mob. Multimed. Networks, WoWMoM 2012 - Digit. Proc., 2012.

[19] J. A. Mahal, A. Khawar, A. Abdelhadi, and T. C. Clancy, "Spectral Coexistence of MIMO Radar and MIMO Cellular System," IEEE Trans. Aerosp. Electron. Syst., vol. 53, no. 2, pp. 655–668, 2017.

[20] J. H. Lim, D. W. Lim, B. L. Cheong, and M. S. Song, "Spectrum Sharing in Weather Radar Networked System: Design and Experimentation," IEEE Sens. J., vol. 19, no. 5, pp. 1720–1729, 2018.

[21] M. Hirzallah and T. Bose, "Steepest descent opportunistic MIMO radar: spectrum sharing design," Analog Integr. Circuits Signal Process., vol. 91, no. 2, pp. 227–237, 2017.

[22] H. Yi, "Nullspace-based secondary joint transceiver scheme for cognitive radio MIMO networks using second-order statistics," IEEE Int. Conf. Commun., 2010.

[23] Y. Noam and A. J. Goldsmith, "Blind null-space learning for spatial coexistence in MIMO cognitive radios," IEEE Int. Conf. Commun., pp. 1726–1731, 2012.

[24] T. Singh and U. Thakur, MIMO Radar, no. May. 2017.

[25] A. Hassanien and S. A. Vorobyov, "Phased-mimo radar: A tradeoff between phased-array and mimo radars," IEEE Trans. Signal Process., vol. 58, no. 6, pp. 3137–3151, 2010.

[26] Q. He, R. S. Blum, H. Godrich, and A. M. Haimovich, "Target velocity estimation and antenna placement for MIMO radar with widely separated antennas," IEEE J. Sel. Top. Signal Process., vol. 4, no. 1, pp. 79–100, 2010.

[27] Sameera P, "Design and Analysis of MIMO Radar GLRT Detector" SSRG International Journal of Electronics and Communication Engineering 2.10 (2015): 34-38.